



**Environmental
Science**
Water Research & Technology

Nutrient Recovery from Treated Wastewater by a Hybrid Electrochemical Sequence Integrating Bipolar Membrane Electrodialysis and Membrane Capacitive Deionization

Journal:	<i>Environmental Science: Water Research & Technology</i>
Manuscript ID	EW-ART-11-2019-000981.R1
Article Type:	Paper

SCHOLARONE™
Manuscripts

Removing nutrient from wastewater is very much needed for reducing the ecological impact of discharge and managing the nutrient cycle. But achieving it sustainably requires minimal use of chemicals and energy. Herein we demonstrate a hybrid electrochemical sequence with minimum chemical use and reasonable energy consumption as a possible way for effective nutrient removal and recovery from wastewater.

1 **Nutrient Recovery from Treated Wastewater by a Hybrid**
2 **Electrochemical Sequence Integrating Bipolar Membrane**
3 **Electrodialysis and Membrane Capacitive Deionization**

4

5

Submitted to the Special Issue of

6

Environmental Science: Water Research and Technology

7

Fei Gao^{a,b,c,#}, Li Wang^{a,#}, Jie Wang^b, Hongwei Zhang^b and Shihong Lin^{*a,d}

8

9 ^a Department of Civil and Environmental Engineering, Vanderbilt University,
10 Nashville, Tennessee 37235-1831, United States

11 ^bState Key Laboratory of Separation Membranes and Membrane Processes, Tianjin
12 Polytechnic University, Tianjin 300387, China

13 ^cSchool of Environmental Science and Engineering, Tianjin University, Tianjin 300072,
14 China

15 ^dDepartment of Chemical and Biomolecular Engineering, Vanderbilt University,
16 Nashville, Tennessee 37235-1604, United States

17 [#]These authors contribute equally.

18

19 Corresponding author: Shihong Lin, shihong.lin@vanderbilt.edu; +1 (615)-322-7226

20

21 ABSTRACT

22 The growing needs for sustainable nutrient management and pollution control have
23 motivated the development of novel technologies for nutrient recovery from wastewater.
24 However, most of the existing technologies require extensive use of chemicals and
25 intensive consumption of energy to achieve substantial recovery of nutrients. Herein,
26 we present a hybrid electrochemical sequence integrating two relatively novel
27 electrochemical processes, bipolar membrane electrodialysis (BMED) and membrane
28 capacitive deionization (MCDI), for simultaneous removal of phosphorus and nitrogen.
29 Specifically, the BMED process is employed to alkalify the wastewater to facilitate
30 struvite precipitation and the MCDI process is used to further reduce the ammonia
31 concentration in the effluent and concentrate the excess ammonia to a small stream.
32 The electrochemical sequence is demonstrated to remove ~89% of the phosphorous and
33 ~77% of ammonia, recovering ~81% of wastewater as high-quality effluent that can be
34 discharged or reused. This electrochemical treatment train minimizes chemical use and
35 has competitive energy consumption as compared to electrochemical processes for
36 nutrient recovery from wastewater.

37

38

39

40

41

42

43

44

45

46

47 1. INTRODUCTION

48 Phosphorus and nitrogen are essential nutrients for agriculture. Phosphorus, as one of
49 most essential resources in society, is currently extracted from non-renewable
50 phosphate reserve and is thus unsustainable¹⁻³. It has been suggested that affordable
51 phosphate reserve will be depleted in foreseeable future unless there is paradigm-shift
52 of the way we manage phosphorous as a resource³⁻⁵. Meanwhile, excessive amount of
53 phosphorus and nitrogen in wastewater need to be removed to protect aquatic
54 ecosystem from eutrophication and to meet growingly stringent discharge regulations⁶⁻
55 ¹¹. To address these challenges, a new paradigm is in need for recovering valuable
56 resources, especially nutrients, from wastewater. The sustainable and cost-effective
57 removal and recovery of $\text{PO}_4^{3-}\text{-P}$ and $\text{NH}_4^+\text{-N}$ from municipal wastewater is of great
58 research interest and societal importance.

59 A notable process that has been heavily investigated in recent years for resource
60 recovery from wastewater is struvite ($\text{MgNH}_4\text{PO}_4 \cdot 6\text{H}_2\text{O}$) precipitation. In this process,
61 both phosphorus and ammonium can be removed and recovered in the form of struvite
62 precipitate which can be used as a slow-release fertilizer^{4, 12, 13}. Precipitation of struvite
63 is sensitive to pH and requires the pH to maintained above 8.5^{14, 15} or even 9.0 when
64 the treated wastewater has a low phosphate-P concentration (e.g., lower than 1 mM)¹⁶.
65 Therefore, the addition of the base is always required to achieve desired pH. In addition,
66 $\text{NH}_4^+\text{-N}$ in typical treated wastewater is stoichiometrically overabundant as compared
67 to $\text{PO}_4^{3-}\text{-P}$. Therefore, struvite precipitation along cannot effective recover all the $\text{PO}_4^{3-}\text{-}$
68 P and $\text{NH}_4^+\text{-N}$ from the treated wastewater. Additional processes are required to further
69 recover and remove the excess $\text{NH}_4^+\text{-N}$ before treated wastewater can be discharged.

70 The motivation behind this study is to develop a treatment train fully based on
71 electrochemical processes to effectively achieve a high degree of $\text{PO}_4^{3-}\text{-P}$ and $\text{NH}_4^+\text{-N}$
72 recovery with the minimum use of the chemicals. The vision of achieving water and
73 wastewater treatment with minimum or even no chemical use is based on the fact that
74 the production of the chemicals often creates additional environmental footprint and the

75 transportation of the chemicals also adds to logistic cost and challenges especially for
76 treatment systems that are distributed and remote. In order to achieve the stated goal,
77 we develop a hybrid electrochemical sequence combining bipolar membrane
78 electro dialysis (BMED) for adjusting the pH for struvite precipitation and membrane
79 capacitive deionization (MCDI) for recovering ammonium. A recent study
80 demonstrates the simultaneous recovery of nitrogen and phosphorus using concurrent
81 flow electrode capacitive deionization (FCDI)¹⁷. This single-stage process focuses on
82 the nutrient removal from the treated water instead of recovering nutrient as fertilizer.

83 Bipolar membrane electro dialysis (BMED) is a relatively novel electro dialysis
84 technology that takes advantage of the special property of a bipolar membrane for
85 splitting water into protons (H^+) and hydroxide ions (OH^-) using an applied voltage¹⁸,
86 ¹⁹. BMED has been explored for generating acidic and alkaline solutions from various
87 electrolytes²⁰⁻²². It has also been integrated with different treatment processes to
88 construct hybrid treatment trains where pH adjustment is required^{23, 24}. For example, it
89 has been coupled with microbial fuel cell (MFC) to produce alkali solution for biogas
90 upgrading²³. It has also been used to acidify seawater for extracting CO_2 from the
91 dissolved carbonate system²⁵. Not only the use of BMED for pH adjustment eliminates
92 the use of chemicals, it can also achieve precise control of pH by varying the current
93 and the hydraulic residence time.

94 The other electrochemical unit process employed in this treatment train is
95 membrane capacitive deionization (MCDI) which has been shown to be effective in
96 separating charged ions from relatively dilute feed water²⁶⁻²⁹. MCDI, or some other
97 variants of capacitive deionization based on activated carbon (AC), such as flow-
98 electrode capacitive deionization³⁰, removes charged ions from water via formation of
99 electrical double layer in the micropores of the AC electrodes. MCDI can be used to
100 recover NH_4^+-N by removing NH_4^+ from a relatively large volume of the feed water,
101 temporarily storing the NH_4^+ ions in the AC electrodes, and later releasing them to a
102 relatively small volume of water as the concentrate rich in NH_4^+-N . In this way, the
103 majority of the feed water has a sufficiently low concentration of NH_4^+-N for discharge

104 or beneficial reuse, whereas the brine has sufficiently high concentration of $\text{NH}_4^+\text{-N}$
105 that can be applied as fertilizer.

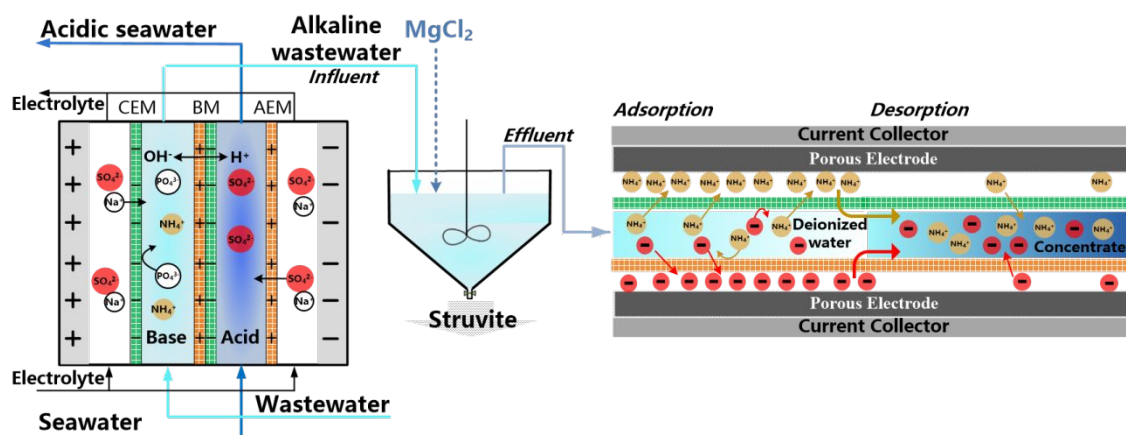
106 In this work, we demonstrate that a hybrid treatment train integrating BMED,
107 struvite precipitation, and multi-stage MCDI for the recovery of phosphorus and
108 ammonium from wastewater. We first investigate the impact of operation parameters
109 in BMED on its performance, and demonstrate that BMED can indeed increase the pH
110 of the wastewater in the alkaline chamber to the desired level for struvite precipitation,
111 while using simulated seawater in the acidic chamber to complete the setup. We then
112 perform a three-stage MCDI process to further remove the ammonium from the
113 supernatant of the wastewater after struvite precipitation and generate a concentrate of
114 ammonium. Finally, the overall performance of the treatment train was assessed in
115 terms of removal efficiency, product water recovery, and energy consumption.

116 **2. MATERIALS AND METHODS**

117 **2.1 Bipolar Membrane Electro-dialysis (BMED) Cell**

118 In this study, we used a lab-scale BMED cell assembled with a cation-exchange
119 membrane (Neosepta CMX, Tokuyama Co., Japan), a bipolar membrane (Fumasep
120 FBM, Fuma-Tech Co., Japan), and an anion-exchange membrane (Neosepta AMX,
121 Tokuyama Co., Japan) placed in parallel as shown (**Fig. 1**). The effective area of each
122 membrane was 17.5 cm^2 . Polypropylene mesh with a thickness of 0.5 mm was used as
123 spacer in each flow channel. Ruthenium-coated titanium electrodes were used in anode
124 and cathode compartments of BMED stack. The BMED cell was operated in a
125 galvanostatic mode as controlled by a potentiostat (SP 150, Bio-Logic, France) that also
126 recorded the real-time system voltage. The simulated wastewater and seawater flowed
127 through the base and acid compartments of the BMED system, respectively, as driven
128 by peristaltic pumps. The electrode rinse solution as pumped through both the anode
129 and cathode compartments. Under the applied electric field, water dissociates within
130 the bipolar membrane (BPM) to generate OH^- ions that enter the base compartment and
131 H^+ ions that enter the acid compartment. In consequence, the seawater and wastewater

132 flowing through the corresponding compartments become acidic and alkaline,
 133 respectively.



134

135 **Fig 1.** Schematic diagram of a lab-scale integrated system for simultaneously removal
 136 and recovery of phosphorus and ammonium in wastewater. The BMED process
 137 increases the pH value of wastewater in the base compartment while acidic seawater
 138 is generated in the acid compartment that decrease the solution. The alkaline
 139 wastewater enters a precipitation reactor for the production of struvite. The effluent
 140 from such a reactor, still rich in NH_4^+ -N, is further treated by a multi-stage MCDI for
 141 NH_4^+ -N recovery.

142

143 2.2 Struvite Precipitation

144 The recovery of phosphorus from wastewater was achieved via the precipitation of
 145 struvite ($MgNH_4PO_4 \cdot 6H_2O$) using the basified wastewater exiting the BMED cell.
 146 $MgCl_2 \cdot 6H_2O$ (analytical grade, Sigma-Aldrich, USA) was added into the precipitator
 147 as the Mg source. The struvite precipitation was carried out in continuously stirred tank
 148 reactor at room temperature (22 ± 1 °C).

149 2.3 Multi-stage Membrane Capacitive Deionization (MCDI) System

150 The multi-stage MCDI system consists of three identical MCDI stacks. Each MCDI
 151 stack has a single-pass flow configuration and is operated using constant (CC) charging
 152 and discharge. The configuration of the MCDI stacks has been described in detail in
 153 previous studies^{27, 31}, and is also given in the Supporting Information. Briefly, four
 154 MCDI assemblies in parallel were housed in an acrylic housing. Each assembly consists

155 of two film electrodes casted with activated carbon particles (PACMM 203, Materials
156 & Methods LLC, Irvine, CA), an AEM, a CEM (both AEM and CEM are the same as
157 those used in BMED), and a glass fiber filter with a thickness of 250 μm (Whatman) as
158 the spacer. Each assembly was cut to a 6 cm \times 6 cm square with a 1.5 cm \times 1.5 cm
159 square hole in the center. The total mass of the four pairs of activated carbon electrodes
160 was 3.06 g. Driven by a peristaltic pump, the feed solution enters through the edge of
161 the stack, flows along the spacer channels, and then exists through the center hole.

162 **2.4 Solution Chemistry and Experimental Procedure**

163 A synthetic wastewater with 2.5 mM PO_4^{3-} and 12.5 mM NH_4^+ was prepared by
164 dissolving inorganic salts of NH_4Cl and $\text{NH}_4\text{H}_2\text{PO}_4$ (analytical grade, Sigma-Aldrich)
165 in MilliQ water. The resulting N:P ratio and concentrations are typical of the
166 supernatant of the secondary sedimentation tank in the municipal wastewater treatment
167 plants^{4, 32}. The model seawater was prepared by adding sea salt (Sigma-Aldrich, USA)
168 to DI water at a concentration of 35 g L^{-1} . The seawater was fed to the acidic chamber
169 to increase the electrical conductivity and reduce the overall cell resistance.

170 In the BMED experiments, a constant volumetric flow rates of 50 ml min^{-1} was
171 used for all streams. We used a semi-batch mode in which the effluent streams from the
172 BMED cell were circulated back to the respective reservoirs of a volume of 500 mL.
173 The seawater and wastewater in the reservoirs thereby became increasingly acidified
174 and alkaline, respectively, which was monitored by measuring the pH in the reservoirs
175 using a pH meter (XL20, Fisher Scientific). The electrode rinse solution (0.1 M Na_2SO_4 ,
176 5L) was circulated through both anode and cathode compartments with a flow rate of
177 150 mL min^{-1} . The experiments were performed at constant current density (10 to 30
178 mA cm^{-2}). For each of the current density, BMED experiments were performed until
179 the target pH for the alkaline wastewater was achieved, and the corresponding operating
180 time and energy consumption (kWh/ m^3) were calculated.

181 Once the pH of the wastewater was raised to the target value, the alkaline
182 wastewater was transferred to a precipitator for struvite precipitation to occur for 8 hr.

183 A semi-batch mode was used in our experiments because of the relatively small size of
184 the BMED cell. In real system with relatively large BMED cell, a single-pass operation
185 mode could be used instead of a semi-batch with recirculation.

186 The supernatant of the precipitation tank was sampled at various time points for
187 composition measurement. The orthophosphate ($\text{PO}_4^{3-}\text{-P}$) and nitrogen ($\text{NH}_4^+\text{-N}$)
188 concentrations were determined using ion chromatography (ICS-2100 IC system,
189 Dionex, CA, USA) and titrimetric method following the Standard Methods (American
190 Public Health Association, 2012), respectively. The precipitate obtained was washed
191 with ultrapure water and dried in an oven at 40°C for 48 h. The dried precipitate was
192 characterized using X-ray diffraction (XRD) (Rigaku Smart Lab, Japan) and compared
193 with standard XRD spectrum for struvite crystal.

194 The effluent from the struvite precipitator was sent to a multi-stage MCDI
195 system for recovery of $\text{NH}_4^+\text{-N}$. In each MCDI cell, the effluent stream in the charging
196 stage (when ions are stored in AC electrodes) is called the deionized water stream, while
197 the effluent stream in the discharge stage (when ions are released to the solution from
198 the AC electrodes) is called the brine stream. In the multi-stage MCDI experiments, the
199 brine stream of the one stage was sent to the next stage as the influent. The deionized
200 water stream from the second MCDI stack was sent to the third MCDI stack as the
201 influent.

202 The $\text{NH}_4^+\text{-N}$ concentration of the effluent streams of the MCDI stacks was
203 continuously measured using an ammonium probe. In each stage, the flow rate was
204 controlled to be 3.5 ml/min, which corresponds to a hydraulic retention time (HRT) of
205 0.96 min. The MCDI experiments were performed with an operation mode of constant
206 current charging and reverse current discharge (CC-RC) as controlled by a potentiostat
207 (SP 150, Bio-Logic, France) that also recorded the real-time cell voltage. In this study,
208 we choose to use different current densities for charging and discharging, both within
209 one stage and between different stages, with the goal of maximizing $\text{NH}_4^+\text{-N}$ removal
210 and achieving water recovery, *WR*.

211 2.5 Data Analysis

212 The following performance metrics were used to evaluate the performance of the unit
 213 processes and the overall sequence. The first performance metric is the specific energy
 214 consumption, SEC_{BMED} (kWh m⁻³), of the BMED process, defined as the energy
 215 consumed to produce a unit volume of the alkaline water. The following expression is
 216 used to calculate SEC_{BMED} :

$$SEC_{BMED} = \frac{\int_0^t U(t) I A_{BM} dt}{V_a} \quad (1)$$

217 where $U(t)$ is the voltage of the BMED cell which is dependent on charging time, t , I is
 218 the applied current density, A_{BM} is the effective area of each bipolar membrane, and
 219 V_a is the volume of alkaline solution produced.

220 In the multi-stage MCDI system, the average effluent and brine NH_4^+ -N
 221 concentrations for the charging and discharging step in each MCDI stage were
 222 calculated based on the following expression:

$$\bar{c} = \frac{\int_0^{t^*} c(t) dt}{t^*} \quad (2)$$

223 where $c(t)$ is the NH_4^+ -N concentration at time t , and t^* is the duration of the
 224 charging or discharge step. Water recovery, WR , is defined as the ratio of volume of
 225 the treated water (or diluted water) to the volume of the feed water in each MCDI stage,
 226 given by

$$WR = \frac{V_d}{V_d + V_b} \quad (3)$$

227 where V_d is the volume of treated water (or diluted water) generated in the charging
 228 step and V_b is the volume of the concentrate (or brine solution) produced in the
 229 discharge step.

230 The energy consumption of the MCDI process is quantified as the energy
 231 consumed to transfer one mole of NH_4^+ -N from the treated water to the concentrate:

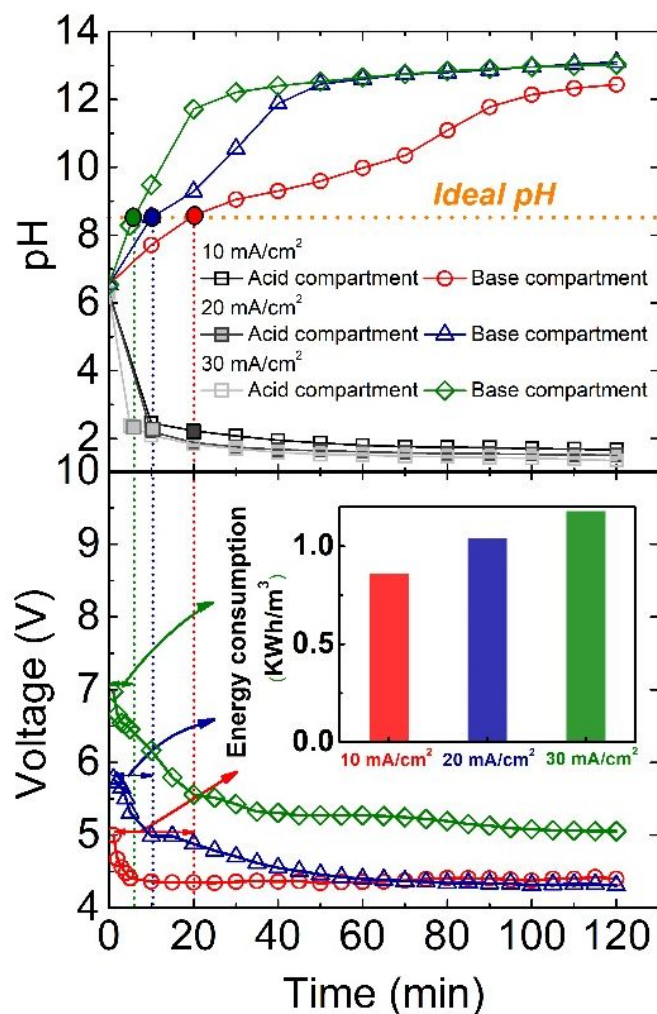
$$SEC_N = \frac{\int_0^t U(t)IA_{IEM}dt}{Q\int_0^t (c_0 - c(t))dt} \quad (4)$$

232 where I is applied current density to the MCDI cell, U is the time-dependent cell voltage
233 response, A_{IEM} is the area of each ion exchange membrane which is also the apparent
234 area of the AC electrode, Q is the flow rate of the MCDI stack, and c_0 is the
235 ammonium concentration in the feed stream.

236 3. RESULTS AND DISCUSSION

237 3.1 Alkalinization of Wastewater by BMED

238 The pH of wastewater increased with time in the BMED process because of the
239 continuous generation of OH^- via water electrolysis in the bipolar membrane (**Fig. 2A**).
240 Naturally, faster increase of pH in the wastewater results from a higher current density
241 that leads to higher production rate of OH^- . To reach the ideal range of pH for struvite
242 precipitation, which is between 8.5 to 9.0, the BMED process was performed for 20, 10
243 and 6 min when the current density was 10, 20 and 30 mA cm^{-2} , respectively.
244 Meanwhile, the pH of the seawater stream dropped to 2.2 ± 0.1 in all cases when the
245 ideal pH range for wastewater was reached. Even though both streams have the same
246 flow rate, the change of pH for the seawater stream was more significant than that for
247 the wastewater stream. The buffering capacity against acidification (i.e. alkalinity) for
248 seawater was lower than the buffering capacity (from PO_4^{3-} and NH_4^+) against
249 alkalinization of wastewater.



250

251 **Fig 2.** The changes of pH changes in acid and base compartments (top) and the
 252 change of voltage of the BMED cell (bottom) as functions of time under different current
 253 densities. The inset shows the specific energy consumption of BMED to adjust the pH
 254 to 8.55 ± 0.05 .

255 Regardless of the current density, cell voltage drop was observed in the course
 256 of the constant current BMED process due to the reduced resistances for both the
 257 seawater and wastewater channels (**Fig. 2B**). The voltage drop was most significant at
 258 the beginning of the BMED process but later leveled off as the acid and base
 259 compartments became more concentrated. Such a trend can be explained by the fact
 260 that the compartment resistance is inversely proportional to electrolyte concentration
 261 and therefore the increase of electrolyte concentration has the strongest impact on
 262 resistance in the range of low electrolyte concentration.

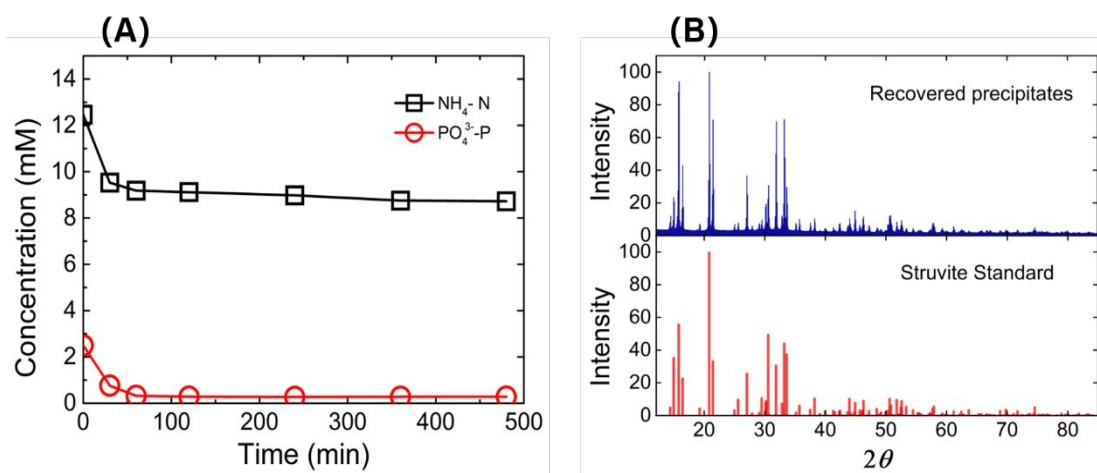
263 The specific energy consumption of BMED, for achieving the target pH of 8.55
264 ± 0.05 in the wastewater increases with current density (**Fig. 2B inset**). There are two
265 major contributions to the energy consumption. First, the process of water electrolysis
266 to generate H^+ and OH^- intrinsically requires minimum energy that corresponds to the
267 Gibbs free energy of the electrochemical conversion. Second, extra energy needs to be
268 provided to drive the process in a finite kinetic rate that is proportional to the current
269 density. For achieving the same pH change of the feed water, the same amount of H^+
270 and OH^- was generated and thus the same amount of Gibbs free energy was thus
271 consumed. However, splitting water at a faster rate requires imposing a higher
272 overpotential to provide a larger driving force, which contributes to the difference in
273 *SEC* at different current densities. In other words, there exists an intrinsic tradeoff
274 between energy efficiency and kinetic rate, that faster alkalization of the wastewater
275 would inevitably consume more energy.

276 **3.2 Struvite Precipitation in Wastewater Effluent from BMED**

277 As shown in Figure 1, the main purpose of the integrated system is to remove and
278 phosphorus and ammonium simultaneously from the wastewater and recover them as
279 nutrients. Phosphorus was recovered from the alkaline wastewater effluent from the
280 BMED cell via the formation of struvite which precipitates from Mg^{2+} , NH_4^+ , and PO_4^{3-} .
281 Both NH_4^+ and PO_4^{3-} already exist in wastewater and the former is typically
282 overabundant as compared to the stoichiometric ratio of struvite. We therefore added
283 Mg^{2+} into the BMED effluent in a 1:1 molar ratio for $Mg^{2+}:PO_4^{3-}$ to initiate the
284 formation of struvite.

285 As a consequence of struvite precipitation, the PO_4^{3-} -P and NH_4^+ -N
286 concentrations of the supernatant decreased over time (**Fig 3A**). The concentration
287 profiles of PO_4^{3-} -P and NH_4^+ -N suggest that the precipitation proceeded to near
288 completion in only 60 min, which is in accordance with the optimal precipitation time
289 for struvite reported by Xu et al¹². There was about 10% of the in the influent to the
290 hybrid treatment train that could not be measured in either the precipitate or the solution,
291 which is likely due to evaporation of NH_3 as reported in reference 33. The phosphate

292 concentration decreased from 2.5 to 0.27 mM, resulting in a phosphate removal
293 efficiency of 89.2%. At the same time, the pH value of supernatant dropped from 8.55
294 ± 0.05 to 8.2 ± 0.1 due to struvite formation. XRD analysis of the composition of the
295 formed precipitate confirms reveals major peaks that are consistent with reference pure
296 struvite crystal standard (**Fig. 3B**).

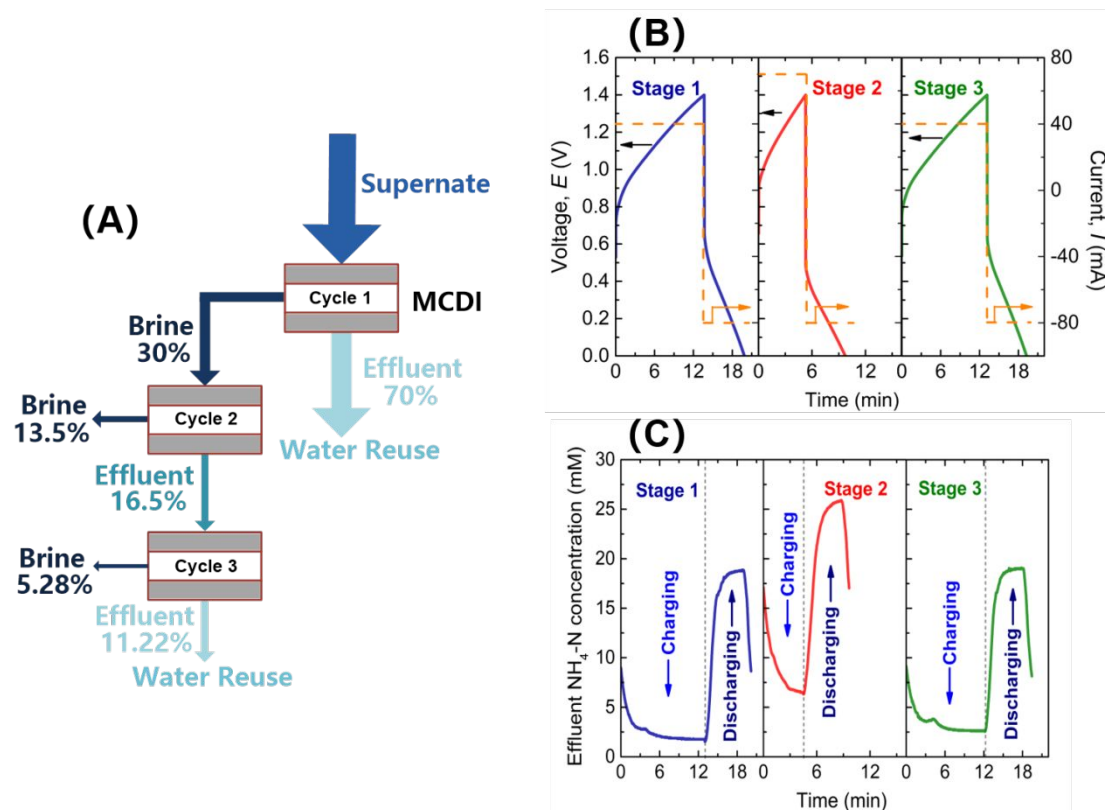


297

298 **Fig. 3** (A) Concentrations of $\text{PO}_4^{3-}\text{-P}$ and $\text{NH}_4^+\text{-N}$ decreased as struvite formed in the
299 precipitator. (B) Powder XRD pattern of the precipitate extracted from the alkaline
300 wastewater in comparison with the standard struvite XRD pattern.

301 3.3 Removal and enrichment of ammonium using multi-stage MCDI

302 Due to the stoichiometric over-abundance of $\text{NH}_4^+\text{-N}$ as compared to $\text{PO}_4^{3-}\text{-P}$, 72%
303 fraction of the $\text{NH}_4^+\text{-N}$ remained in the supernatant upon the completion of the struvite
304 precipitation (**Fig 3A**). To further reduce the effluent $\text{NH}_4^+\text{-N}$ concentration for meeting
305 discharge standard and for recovering $\text{NH}_4^+\text{-N}$ as a valuable nutrient, we used a multi-
306 stage MCDI process to obtain a solution with enriched $\text{NH}_4^+\text{-N}$. Extensive experiments
307 with a variety of operating conditions (e.g. the current and flowrate of the charging and
308 discharge stages) have been tested to optimize this multi-stage MCDI process, with
309 results only from the optimal operating conditions presented in the following discussion.



310

311 **Fig 4.** (A) A schematic diagram of a three-stage MCDI process in which the
 312 concentrated brine from the first stage is sent as the feed stream to a two-stage MCDI
 313 process for further extraction of ammonia nitrogen. This three-stage process enables
 314 a high WR with effluent of low $\text{NH}_4^+\text{-N}$ concentration. (B) cell current and voltage, and
 315 (C) effluent $\text{NH}_4^+\text{-N}$ concentration as functions of time in the charging and discharge
 316 steps at different stages. The water flowrate is 3.5 mL min^{-1} .

317 The three-stage MCDI process was operated as following: the supernatant from
 318 struvite precipitator, rich in $\text{NH}_4^+\text{-N}$, was fed to the first stage MCDI as the feed water
 319 (**Fig. 4A**). In this first stage, the water recovery was 70% and the $\text{NH}_4^+\text{-N}$ concentration
 320 of treated effluent was $\sim 2.5 \text{ mM}$ (**Fig. 4B**). The brine of the first stage was then sent to
 321 the second stage which recovered 55% of the second stage influent (i.e., 16.5% of the
 322 overall influent). The average $\text{NH}_4^+\text{-N}$ concentration of treated effluent in the second
 323 stage was $\sim 15.6 \text{ mM}$, which was still too high for direct discharge. Therefore, the
 324 treated effluent in the second stage MCDI was further subject to a third stage MCDI
 325 separation. The water recovery of the third stage MCDI process was 68%, which was
 326 $\sim 11.2\%$ of the influent to the multi-stage MCDI system. The average $\text{NH}_4^+\text{-N}$
 327 concentration of the treated effluent in the third stage was $\sim 4.6 \text{ mM}$.

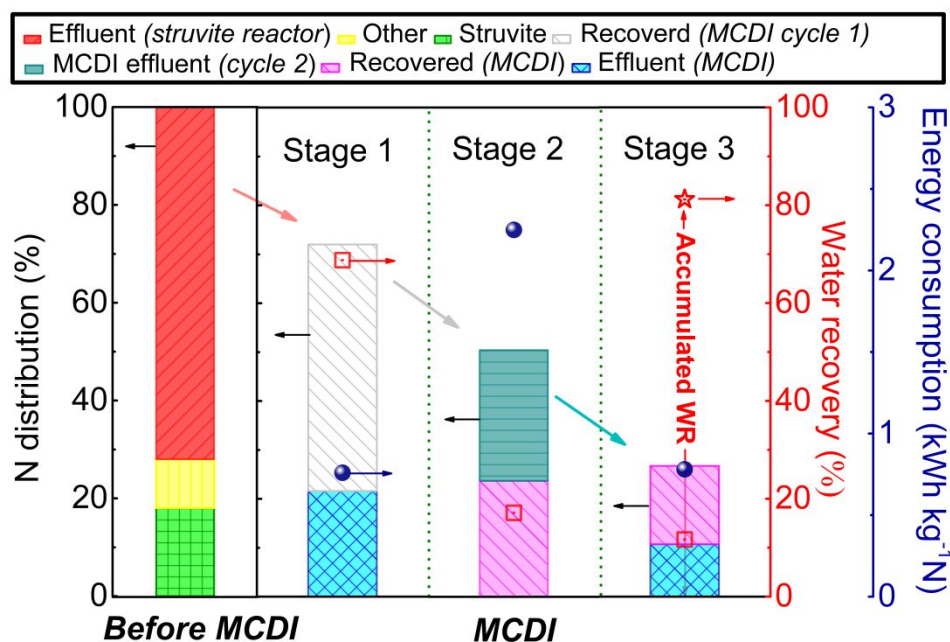
328 In each stage, the MCDI cell was operated using constant current charging and
329 reverse current discharge (i.e. a CC-RC mode). The charging current was 40 mA in the
330 first and third stage, and was 70 mA in the second stage due to the higher influent
331 concentration of $\text{NH}_4^+\text{-N}$. The discharge current was 80 mA in all stages (**Fig. 4C**). The
332 flow rate was maintained at 3.5 mL min^{-1} for both charging and discharge in all stages.
333 We chose to terminate charging when the cell voltage reached 1.4V (to prevent
334 electrolysis of water) and to terminate discharge when the cell voltage reached zero.
335 With this specific operation criterion, the charging-discharge cycle was shorter in the
336 second stage with a higher charging current. Specifically, the full charging-discharge
337 cycle for the second stage is about half of that for the first and third stages.

338 If we define removal efficiency as the percentage reduction of the feed
339 concentration (in the product water) and the enrichment efficiency as ratio between the
340 brine concentration and feed concentration, the first and third stage MCDI achieved an
341 $\text{NH}_4^+\text{-N}$ removal efficiency of 72% and an enrichment factor of ~ 1.9 , whereas the
342 second stage MCDI achieved an $\text{NH}_4^+\text{-N}$ removal efficiency of $\sim 47\%$ and an
343 enrichment efficiency of ~ 1.4 . Overall, the three-stage MCDI process recovered over
344 81.2% of the effluent of the struvite precipitator with $\text{NH}_4^+\text{-N}$ removal efficiency of
345 72%. It also generated $\sim 18.8\%$ of concentrated $\text{NH}_4^+\text{-N}$ solution with an overall
346 enrichment factor of ~ 1.8 .

347 The $\text{NH}_4^+\text{-N}$ distribution throughout the treatment train and the performance
348 metrics for each MCDI stage are summarized in **Fig. 5**. The majority (72%) of the
349 $\text{NH}_4^+\text{-N}$ remained in the effluent of the struvite precipitator, and 18% of the $\text{NH}_4^+\text{-N}$
350 was removed in formed struvite. There was about 10% of the $\text{NH}_4^+\text{-N}$ in the influent to
351 the hybrid treatment train that could not be measured in either the precipitate or the
352 solution, which is likely due to evaporation of NH_3 as reported in literature³³. The $\text{NH}_4^+\text{-N}$
353 N accounting suggests that the first stage MCDI process alone could remove 72% of
354 the $\text{NH}_4^+\text{-N}$ in the influent stream and recover 70% of water. Notably, the first stage
355 MCDI process also consumed the least energy ($1.87 \text{ kWh kg}^{-1} \text{ N}$).

356 However, further enhancing water recovery becomes increasingly difficult. The
 357 second and third stages combined only recovered ~12% more water while consuming
 358 much more energy for $\text{NH}_4^+\text{-N}$ removal. Specifically, the second and third stages
 359 consumed 2.80 and 2.11 $\text{kWh kg}^{-1} \text{N}$, respectively. With the tested flow rate and the
 360 same level of $\text{NH}_4^+\text{-N}$ removal, the total treatment time for achieving 82% water
 361 recovery was 49 min, which is nearly two and half longer than achieving a water
 362 recovery of 70%. Therefore, there is a diminishing return in both the aspects of energy
 363 consumption and kinetics when the MCDI system was challenged to achieve a higher
 364 water recovery.

365



366

367 **Fig 5.** Distribution of $\text{NH}_4^+\text{-N}$ (bar), water recovery (red square), and specific energy
 368 consumption (blue circle) in the electrochemical sequence. The hybrid process
 369 recovers 82% water, removes ~100% $\text{PO}_4^{3-}\text{-P}$ in the form of struvite and 77 % of the
 370 $\text{NH}_4^+\text{-N}$ in the forms of both struvite and $\text{NH}_4^+\text{-N}$ concentrate.

371 The overall process of the MCDI was to generate two diluted streams and two
 372 brine streams. The energy requirement of the three-stage MCDI system was 3.22 kWh
 373 $\text{kg}^{-1} \text{N}$ that is consumed to concentrate N from the precipitation supernatant (feed) to
 374 the brine of the MCDI system, which is very competitive with other $\text{NH}_4^+\text{-N}$

375 removal/recovery technologies. For instance, energy requirement for NH_4^+ -N removal
376 by the conventional activated sludge process (based on nitrification and denitrification)
377 ranges from 6.18-13.6 kWh kg^{-1} N³⁴. When combined microbial and electrochemical
378 process, namely bio-electrochemical system (BES) and BES-based system with the
379 representative examples as microbial fuel cell and microbial electrolysis cell, ammonia
380 may be removed and recovered with much lower energy consumption³⁵⁻³⁷. However,
381 biological processes still require long start-up time and are sensitive to environmental
382 factors (e.g. pH, temperature and influent quality)³⁸. The three-stage MCDI process
383 reported in this study also consumed less energy when compared with FCDI or FCDI-
384 based processes that have been reported to consume 6.1~21.7 kWh kg^{-1} N^{33, 39}.

385 **4. CONCLUSIONS**

386 We have demonstrated an integrated system that incorporates BMED, struvite reactor
387 and multi-stage MCDI in sequence. This system with two major electrochemical
388 components, BMED and MCDI, enables efficient removal and recovery (enrichment)
389 of nutrients from wastewater with the minimal use of chemicals. While the economic
390 competitiveness of BMED as compared to chemical dosing for pH adjustment requires
391 more extensive techno-economic analysis, BMED as an alternative for pH adjustment
392 converts the chemical consumption to energy consumption and thus can potentially be
393 powered by sustainable energy. The prevention of using chemicals for pH adjustment
394 is also beneficial to the subsequent removal of NH_4^+ , because it reduces the amount of
395 counter ions (anions in this case) in the feed water entering the MCDI system, which
396 reduces the competitive adsorption of other cations vs. NH_4^+ and thereby reduces
397 energy consumption for NH_4^+ recovery.

398 The proposed electro-chemical sequence also has a high adaptability to different
399 source water and target water quality. While we use treated wastewater as an example
400 in this study, the electro-chemical sequence may also be used for efficient removal and
401 recovery (enrichment) of nutrients from feed streams of high nutrient concentrations
402 and large N/P ratio (>10, e.g. urine and pig manure). The two major operating

403 parameters, including applied current density and hydraulic residence time can be tuned
404 simultaneously to achieve the target treatment goal.

405

406 **ACKNOWLEDGEMENT**

407 F.G acknowledges the support from the China Scholarship Council (201806250113).

408 L.W. and S.L. acknowledge the support by the Natural Science Foundation via research
409 grant 1739884.

410

411 **REFERNCES**

- 412 1. P. Falkowski, R. J. Scholes, E. Boyle, J. Canadell, D. Canfield, J. Elser, N. Gruber, K. Hibbard, P.
413 Hogberg, S. Linder, F. T. Mackenzie, B. Moore, T. Pedersen, Y. Rosenthal, S. Seitzinger, V.
414 Smetacek and W. Steffen, The global carbon cycle: A test of our knowledge of earth as a system,
415 *Science*, 2000, **290**, 291-296.
- 416 2. D. Cordell, A. Rosemarin, J. J. Schroder and A. L. Smit, Towards global phosphorus security: A
417 systems framework for phosphorus recovery and reuse options, *Chemosphere*, 2011, **84**, 747-
418 758.
- 419 3. Y. Zhang, E. Desmidt, A. Van Looveren, L. Pinoy, B. Meesschaert and B. Van der Bruggen,
420 Phosphate Separation and Recovery from Wastewater by Novel Electrodialysis, *Environ Sci*
421 *Technol*, 2013, **47**, 5888-5895.
- 422 4. S. H. Lee, B. H. Yoo, S. K. Kim, S. J. Lim, J. Y. Kim and T. H. Kim, Enhancement of struvite purity
423 by re-dissolution of calcium ions in synthetic wastewaters, *J Hazard Mater*, 2013, **261**, 29-37.
- 424 5. J. Driver, D. Lijmbach and I. Steen, Why recover phosphorus for recycling, and how?,
425 *Environmental technology*, 1999, **20**, 651-662.
- 426 6. R. D. Schuilting and A. Andrade, Recovery of struvite from calf manure, *Environmental*
427 *technology*, 1999, **20**, 765-768.
- 428 7. D. J. Conley, H. W. Paerl, R. W. Howarth, D. F. Boesch, S. P. Seitzinger, K. E. Havens, C. Lancelot
429 and G. E. Likens, Controlling Eutrophication: Nitrogen and Phosphorus, *Science*, 2009, **323**,
430 1014.
- 431 8. S. Agrawal, J. S. Guest and R. D. Cusick, Elucidating the impacts of initial supersaturation and
432 seed crystal loading on struvite precipitation kinetics, fines production, and crystal growth,
433 *Water Res*, 2018, **132**, 252-259.
- 434 9. J. Jack, T. M. Huggins, Y. P. Huang, Y. F. Fang and Z. J. Ren, Production of magnetic biochar from
435 waste-derived fungal biomass for phosphorus removal and recovery, *J Clean Prod*, 2019, **224**,
436 100-106.

- 437 10. N. Zhao, H. Wang, Z. He and Q. Yan, Ammonia removal and recovery from diluted forward
438 osmosis draw solution by using a tubular microbial desalination cell, *Environ Sci-Wat Res*, 2019,
439 **5**, 224-230.
- 440 11. M. H. Qin, E. A. Hynes, I. M. Abu-Reesh and Z. He, Ammonium removal from synthetic
441 wastewater promoted by current generation and water flux in an osmotic microbial fuel cell,
442 *J Clean Prod*, 2017, **149**, 856-862.
- 443 12. K. N. Xu, J. Y. Li, M. Zheng, C. Zhang, T. Xie and C. W. Wang, The precipitation of magnesium
444 potassium phosphate hexahydrate for P and K recovery from synthetic urine, *Water Res*, 2015,
445 **80**, 71-79.
- 446 13. L. T. Angenent, K. Karim, M. H. Al-Dahhan and R. Domiguez-Espinosa, Production of bioenergy
447 and biochemicals from industrial and agricultural wastewater, *Trends Biotechnol*, 2004, **22**,
448 477-485.
- 449 14. J. D. Doyle and S. A. Parsons, Struvite formation, control and recovery, *Water Res*, 2002, **36**,
450 3925-3940.
- 451 15. Y. H. Song, G. L. Qiu, P. Yuan, X. Y. Cui, J. F. Peng, P. Zeng, L. Duan, L. C. Xiang and F. Qian,
452 Nutrients removal and recovery from anaerobically digested swine wastewater by struvite
453 crystallization without chemical additions, *J Hazard Mater*, 2011, **190**, 140-149.
- 454 16. A. Adnan, M. Dastur, D. S. Mavinic and F. A. Koch, Preliminary investigation into factors
455 affecting controlled struvite crystallization at the bench scale, *J Environ Eng Sci*, 2004, **3**, 195-
456 202.
- 457 17. Y. H. Bian, X. Chen, L. Lu, P. Liang and Z. J. Ren, Concurrent Nitrogen and Phosphorus Recovery
458 Using Flow-Electrode Capacitive Deionization, *Acs Sustain Chem Eng*, 2019, **7**, 7844-7850.
- 459 18. Y. C. Chiao, F. P. Chlanda and K. N. Mani, Bipolar Membranes for Purification of Acids and Bases,
460 *J Membrane Sci*, 1991, **61**, 239-252.
- 461 19. S. Mafe, P. Ramirez and A. Alcaraz, Electric field-assisted proton transfer and water
462 dissociation at the junction of a fixed-charge bipolar membrane, *Chem Phys Lett*, 1998, **294**,
463 406-412.
- 464 20. Y. Y. Chen, J. R. Davis, C. H. Nguyen, J. C. Baygents and J. Farrell, Electrochemical Ion-Exchange
465 Regeneration and Fluidized Bed Crystallization for Zero-Liquid-Discharge Water Softening,
466 *Environ Sci Technol*, 2016, **50**, 5900-5907.
- 467 21. L. Shi, Y. S. Hu, S. H. Xie, G. X. Wu, Z. H. Hu and X. M. Zhan, Recovery of nutrients and volatile
468 fatty acids from pig manure hydrolysate using two-stage bipolar membrane electrodialysis,
469 *Chem Eng J*, 2018, **334**, 134-142.
- 470 22. Y. M. Zhou, H. Y. Yan, X. L. Wang, Y. M. Wang and T. W. Xu, A closed loop production of water
471 insoluble organic acid using bipolar membranes electrodialysis (BMED), *J Membrane Sci*, 2016,
472 **520**, 345-353.
- 473 23. M. Chen, F. Zhang, Y. Zhang and R. J. Zeng, Alkali production from bipolar membrane
474 electrodialysis powered by microbial fuel cell and application for biogas upgrading, *Appl Energy*,
475 2013, **103**, 428-434.
- 476 24. S. Mikhaylin, L. Patouillard, M. Margni and L. Bazinet, Milk protein production by a more
477 environmentally sustainable process: bipolar membrane electrodialysis coupled with
478 ultrafiltration, *Green Chem*, 2018, **20**, 449-456.

- 479 25. M. D. Eisaman, K. Parajuly, A. Tuganov, C. Eldershaw, N. R. Chang and K. A. Littau, CO₂
480 extraction from seawater using bipolar membrane electrodialysis, *Energ Environ Sci*, 2012, **5**,
481 7346-7352.
- 482 26. S. Porada, R. Zhao, A. van der Wal, V. Presser and P. M. Biesheuvel, Review on the science and
483 technology of water desalination by capacitive deionization, *Prog Mater Sci*, 2013, **58**, 1388-
484 1442.
- 485 27. L. Wang and S. H. Lin, Membrane Capacitive Deionization with Constant Current vs Constant
486 Voltage Charging: Which Is Better?, *Environ Sci Technol*, 2018, **52**, 4051-4060.
- 487 28. L. Wang and S. H. Lin, Theoretical framework for designing a desalination plant based on
488 membrane capacitive deionization, *Water Res*, 2019, **158**, 359-369.
- 489 29. Z. Ge, X. Chen, X. Huang and Z. Y. J. S. Ren, Capacitive deionization for nutrient recovery from
490 wastewater with disinfection capability, *Environ Sci-Wat Res*, 2018, **4**, 33-39.
- 491 30. S. I. Jeon, H. R. Park, J. G. Yeo, S. Yang, C. H. Cho, M. H. Han and D. K. Kim, Desalination via a
492 new membrane capacitive deionization process utilizing flow-electrodes, *Energ Environ Sci*,
493 2013, **6**, 1471-1475.
- 494 31. L. Wang and S. H. Lin, Mechanism of Selective Ion Removal in Membrane Capacitive
495 Deionization for Water Softening, *Environ Sci Technol*, 2019, **53**, 5797-5804.
- 496 32. A. J. Ward, K. Arola, E. T. Brewster, C. M. Mehta and D. J. Batstone, Nutrient recovery from
497 wastewater through pilot scale electrodialysis, *Water Res*, 2018, **135**, 57-65.
- 498 33. C. Y. Zhang, J. X. Ma, D. He and T. D. Waite, Capacitive Membrane Stripping for Ammonia
499 Recovery (CapAmm) from Dilute Wastewaters, *Environ Sci Tech Let*, 2018, **5**, 43-49.
- 500 34. M. Maurer, P. Schwegler and T. A. Larsen, Nutrients in urine: energetic aspects of removal and
501 recovery, *Water Sci Technol*, 2003, **48**, 37-46.
- 502 35. P. Kuntke, K. M. Smiech, H. Bruning, G. Zeeman, M. Saakes, T. H. J. A. Sleutels, H. V. M.
503 Hamelers and C. J. N. Buisman, Ammonium recovery and energy production from urine by a
504 microbial fuel cell, *Water Res*, 2012, **46**, 2627-2636.
- 505 36. Y. F. Zhang and I. Angelidaki, Recovery of ammonia and sulfate from waste streams and
506 bioenergy production via bipolar bioelectrodialysis, *Water Res*, 2015, **85**, 177-184.
- 507 37. P. Zamora, T. Georgieva, A. Ter Heijne, T. H. J. A. Sleutels, A. W. Jeremiasse, M. Saakes, C. J. N.
508 Buisman and P. Kuntke, Ammonia recovery from urine in a scaled-up Microbial Electrolysis Cell,
509 *J Power Sources*, 2017, **356**, 491-499.
- 510 38. Y. F. Zhang and I. Angelidaki, Submersible microbial desalination cell for simultaneous
511 ammonia recovery and electricity production from anaerobic reactors containing high levels
512 of ammonia, *Bioresource Technol*, 2015, **177**, 233-239.
- 513 39. C. Y. Zhang, J. X. Ma, J. K. Song, C. He and T. D. Waite, Continuous Ammonia Recovery from
514 Wastewaters Using an Integrated Capacitive Flow Electrode Membrane Stripping System,
515 *Environ Sci Technol*, 2018, **52**, 14275-14285.

516